Purdue University

## Purdue e-Pubs

International Compressor Engineering
Conference

School of Mechanical Engineering

2022

# An Improved Mass Flow Rate Prediction Method for Rolling Piston Compressors

ChengYi Lee

Yunho Hwang

Scott Shaffer

Follow this and additional works at: https://docs.lib.purdue.edu/icec

# An Improved Mass Flow Rate Prediction Method for Rolling Piston Compressors

Cheng-Yi Lee[1], Yunho Hwang[1*], Scott Shaffer[2]

[1]Center for Environmental Energy Engineering, Department of Mechanical Engineering, University of Maryland, 4164 Glenn Martin Hall Bldg., College Park, MD 20742, United States

[2]GE Appliances, Appliance Park, Louisville, KY 40225-0001, United States

* Corresponding Author: Tel: (301) 405-5247, email: yhhwang@umd.edu

## ABSTRACT

An improved mass flow rate prediction method for rolling piston-type compressors was proposed. The critical parameters affecting the mixture leakage across the clearance were identified by deriving the governing equation of refrigerant mixture leakage inside the compression chamber. By correlating with the experimental reference test point, the geometry of the compression chamber can be ignored, and the refrigerant loss was only related to the mixture leakage from the compression side to the suction side. The volumetric efficiency can be predicted using the experimental result of a reference test point with solubility and kinematic viscosity data. A compressor test facility was built to measure the compressor mass flow rate under a wide range of testing conditions. The mixture temperature of the reference test point was assigned. For one reference point prediction, there are 34% data within a 5% deviation and 66% data within a 10% deviation. The prediction accuracy improved to 57% within a 5% deviation and 84% within a 10% deviation for two points prediction. Then, based on the regression data of the discharge temperature, an oil-sump temperature equation as a function of condensing temperature was derived. The single-point prediction accuracy even outperforms the manufacturer's map to 81% within a 5% deviation and 100% within a 10% deviation.

## 1. INTRODUCTION

The feature of rolling piston compressors has been widely utilized for domestic air conditioners and heat pumps for several decades. Its intrinsic properties, such as low noise, high efficiency, lightweight, or fewer component assembly, make manufacturers and researchers continuously interested in improving it (Li et al., 2021).

One of the major concerns for the air conditioners and heat pumps manufacturers was that the compressor performance map from compressor suppliers was often inaccurately predicting the performance, especially under low ambient temperature conditions. Lee et al. (2021) observed that the mass flow rate of a fixed-speed rotary compressor could deviate from the provided compressor map up to 63% under the low ambient temperature condition tests. Inspired by the currently limited prediction capability, this work aims at generating a comprehensive performance map through one or two experimental test points by identifying the critical factors affecting volumetric efficiency.

The rolling piston compressor can be treated as an oil-flooded compressor (Huff, 2003). The refrigerant leakage through the clearance between roller and cylinder is the main contribution to the volumetric efficiency loss. Costa et al. (1990) conducted a flow visualization experiment of the refrigerant-oil mixture inside the radial clearance of a rolling piston compressor. They found out the radial clearance was well sealed with the refrigerant-oil mixture, and once the flow entered the downstream, it turned into the two-phase flow. This observed phenomenon motivated researchers to simulate and experiment with the variated oil mixture through the radial clearance (Castro and Gasche, 2006., Poiate and Gasche, 2006., Dias et al., 2011., Gasche et al., 2012., Cai et al., 2015., Cai et al., 2017). Cai et al. (2017) proposed a mathematical model to predict the volumetric efficiency of rolling piston compressors by analyzing the impact of minimal clearance, pressure difference, length, and geometry of the leakage channel.

In industry, compressor manufacturers follow the AHRI Standard 540 (2020), which provides a 10-coefficient cubic polynomial model to predict mass flow rates, power consumption, etc. At least 10 test points are needed to generate a 10-coefficient model, and more data points are required for better prediction capability. This study investigated

and identified the crucial factors that affect refrigerant-oil leakage inside the compression chamber based on the governing equations. Hence, the internal leakage properties of the refrigerant-oil mixture can be correlated with the experimental test data to accurately predict the mass flow rate.

## 2. LEAKAGE MODEL

Many researchers have modeled refrigerant leakage through different approaches. Some authors modeled the leakage as compressible pure refrigerant gas flow (Yanagisawa and Shimisu, 1985); Others consider it a mixture of lubricating oil and refrigerant (Lee and Min, 1988). The flow visualization experiment performed by Costa et al. (1990) further confirmed the latter assumption. In the observation, the oil-refrigerant mixture well sealed the clearance and turned into the two-phase flow downstream. Hence, it can be inferred that the refrigerant leakage comes from the refrigerant oil mixture's solubility difference between the compression chamber and suction chamber.

### 2.1 Governing Equation

A leakage simulation model proposed by Cai et al. (2015) investigated the four leakage paths inside the compression chamber, including the leakage through radial clearance (1), clearances between the rolling piston faces and the cylinder head walls (2), clearances between the sides of the sliding vane (3) and the sidewalls of the chutes inside the cylinder (4), as shown in Figure 1. For a steady-state, incompressible, viscous laminar flow, the continuity and momentum equations are shown in equations (1) and (2).

$$\frac{\partial(\rho u)}{\partial x} + \frac{\partial(\rho v)}{\partial y} = 0 \tag{1}$$

$$\rho(u\frac{\partial u}{\partial x} + v\frac{\partial u}{\partial y}) = -\frac{dp}{dx} + \mu\frac{\partial^2 u}{\partial y^2} \tag{2}$$

The density term in Eq. (1) can be removed because of the incompressible condition. For the non-slip wall boundary condition, $\partial u / \partial x = 0$ then we can derive $\partial v / \partial y = 0$ from Eq. (1). Then, Eq. (2) can be simplified as follows:

$$0 = -\frac{dp}{dx} + \mu\frac{\partial^2 u}{\partial y^2} \tag{3}$$
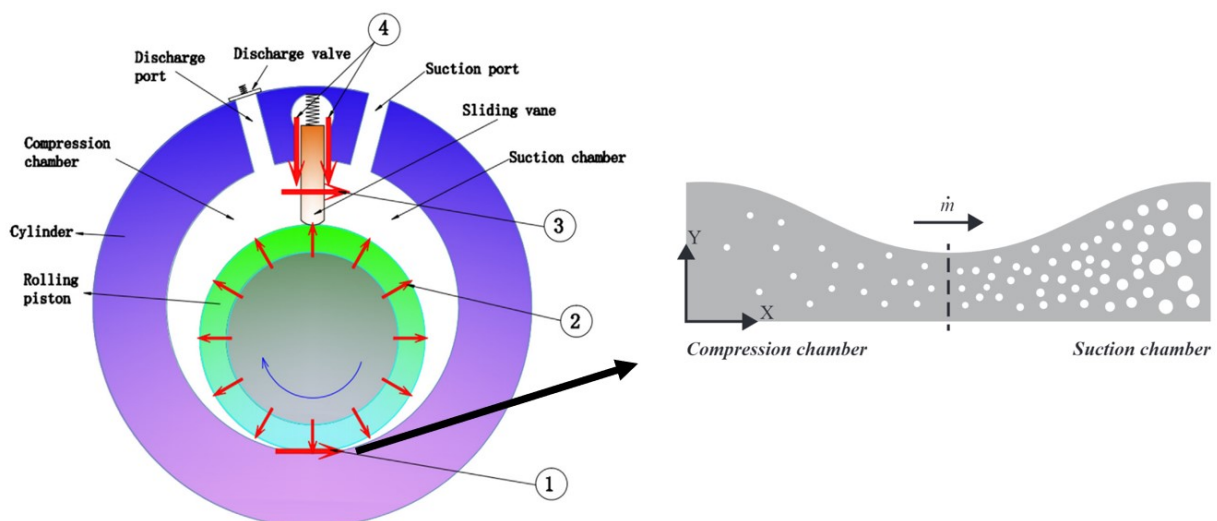


**Figure 1:** Leakage paths of a rolling piston type compressor (Cai et al., 2015)

From Eq. (3), we can quickly determine that the leakage flow velocity is proportional to the pressure difference and inversely proportional to kinematic viscosity, as shown in Eq. (4). In addition, geometry terms x and y are used to describe the different leakage paths based on the clearance geometry. Some researchers consider the leakage induced by wall velocity as part of leakage losses and assume it can be added linearly with leakage loss caused by the pressure difference (Wu., 2000, Yang et al., 2011). However, it is not easy to quantify each portion of mixture leakage, and more experimental works are needed to investigate the mechanism between leakage caused by pressure difference and wall velocity. Hence, this work only considers the pressure difference as the leakage driving force of the refrigerant oil mixture.

$$\dot{m}_{oil\ mixure} \propto \frac{\triangle P}{\nu_{(T,P)}} \tag{4}$$

Since we are testing a particular compressor and predicting the mass flow rate based on its data, the geometry term can be negligible in predicting the refrigerant oil mixture's mass flow rate. Therefore, once we have a reference test point, we can predict the mass flow rate at any given condition according to the pressure difference between discharge pressure and suction pressure and the kinematic viscosity, as Eq. (5) shows.

$$\dot{m}_{oil\ mixure,P} = \dot{m}_{oil\ mixure,R} \times \frac{\triangle P_P}{\triangle P_R} \times \frac{\overline{\nu_{R(T,P)}}}{\overline{\nu_{P(T,P)}}} \tag{5}$$

## 2.2 Physical and Thermodynamic Properties

An accurate refrigerant oil mixture properties data is essential to predict the mass flow rate. The refrigerant/lubricant properties correlations made by Henderson (1994) were utilized in this work. Eq. (6) and Eq. (7) show the vapor and kinematic equation as a function of temperature (T) and solubility ($\omega$) for the range $0 < T < 75°C$. These two equations are utilized to calculate the solubility and kinematic viscosity of the refrigerant mixture. The corresponding coefficients are listed in Table 1. On top of that, the R410A suction density was calculated through EES: Engineering Equation Solver.

$$P = (a_1 + a_2 T + a_3 T^2) + \omega(a_4 + a_5 T + a_6 T^2) + \omega^2(a_7 + a_8 T + a_9 T^2) \tag{6}$$

$$\log(\log(v + 0.7)) = (a_1 + a_2 \log(T) + a_3 \log^2(T)) + \omega(a_4 + a_5 \log(T) + a_6 \log^2(T)) \\ + \omega^2(a_7 + a_8 \log(T) + a_9 \log^2(T)) \tag{7}$$

**Table 1:** Coefficients of R32/POE 68 and R125/POE 68 refrigerant/lubricant mixtures

| Coefficients | Vapor pressure R32/POE 68 | Vapor pressure R125/POE 68 | Kinematic viscosity R32/POE 68 | Kinematic viscosity R125/POE 68 |
|---|---|---|---|---|
| $a_1$ | 5.23901E+2 | 2.01910E+3 | 8.73084 | 8.62420 |
| $a_2$ | -4.07248 | -1.25159E+1 | -3.38970 | -3.34716 |
| $a_3$ | 8.03095E-3 | 1.92469E-2 | 0 | 0 |
| $a_4$ | 1.17981E+4 | 6.00305E+4 | -1.70416 | 1.14890E+1 |
| $a_5$ | -2.41853E+2 | -5.19229E+2 | -1.11362E-2 | -4.87541 |
| $a_6$ | 7.72624E-1 | 1.11454 | 0 | 0 |
| $a_7$ | 5.99182E+4 | -5.30431E+4 | 1.22241E+1 | -3.42108E+1 |
| $a_8$ | -9.18687E+1 | 4.86166E+2 | -4.69226 | 1.32973E+1 |
| $a_9$ | -5.20589E-1 | -1.00753 | 0 | 0 |
| $\sigma$ | 0.9959 | 0.9995 | 0.9998 | 0.9995 |

R410A(R32/R125, 50/50 wt.%) refrigerant is a near-azeotropic mixture. And we assumed the refrigerant oil mixture is saturated at the inlet and outlet of the leakage path. The solubility can be obtained by applying the R410A vapor pressure and refrigerant oil mixture temperature as inputs in Eq. (6). Then the kinematic viscosity of R32/POE68 and R125/POE68 can be derived from Eq. (7). By applying the Kendall-Monroe equation (8), the binary mixture's kinematic viscosity can be calculated. In Eq. (8), α represents the mass fraction in the mixture.

$$\nu_{oil\ mixture} = (\alpha_1 \nu_{R32/POE68}^{1/3} + \alpha_2 \nu_{R125/POE68}^{1/3})^3 \tag{8}$$

The visualization experiment done by Costa et al. (1990) demonstrated the upstream single-phase flow transfer into the two-phase flow downstream. When the high-pressure saturated mixture passes through the clearance, it encounters a pressure drop that decreases the solubility. The outgassed refrigerant absorbed the heat from the mixture and changed the density and viscosity accordingly. Such a non-isothermal model is proposed by Dias et al. (2011) and Gasche et al. (2012) to describe the leakage behavior. Gasche et al. (2012) pointed out that the mass flow rate prediction difference between isothermal and non-isothermal models can reach 11% for the larger pressure drop case. However, we still adopted the isothermal model because of its simplicity. In addition, their works show that the reference test point shouldn't be far from the prediction point in terms of pressure difference to avoid the property change caused by the pressure drop.

## 3. TEST FACILITY

The compressor test stand was developed based on the hot gas bypass method. The testing capacity of the compressor test stand ranged from 0.58 kW to 7.3 kW. Figure 2 shows the schematic of the compressor test stand. The mass flow meter measuring the total refrigerant flow was placed right after the discharge port. There were two pairs of RTD and pressure transducers to monitor the discharge and suction temperature and pressure. The electric expansion valve1 can control the discharge pressure to desired operating conditions. Then the refrigerant flows split into two paths. One direct bypass and expanded to suction pressure. The other was condensed by a chiller at a constant temperature, then expanded to suction conditions. The EEV2 and EEV3 worked together to obtain the target suction pressure and superheat.
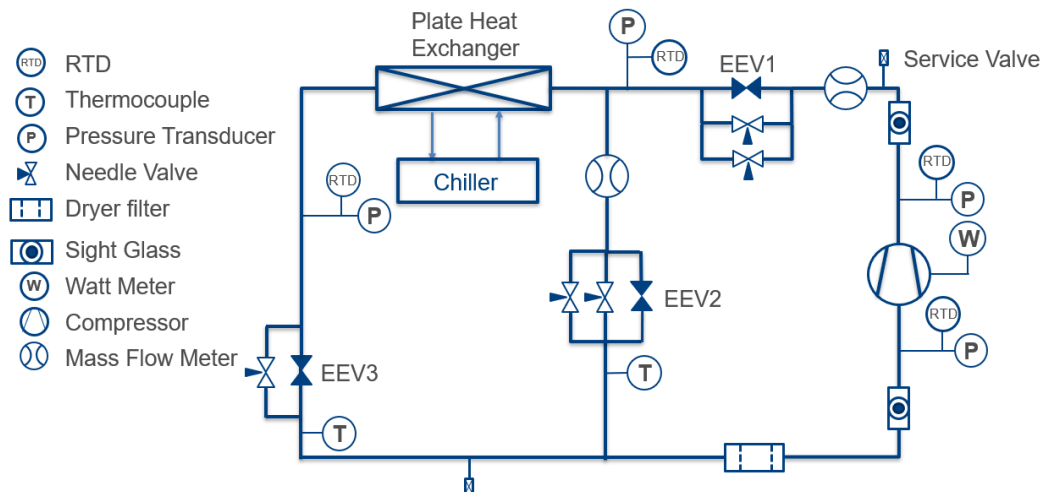


**Figure 2:** Test facility schematic diagram

### 3.1 Instruments and Uncertainties

Table 2 lists the instrument used in our compressor test facility. The compressor discharge and suction temperature were measured by using the RTD sensor. The T-type thermocouples were placed over the entire system to monitor the system's overall behavior, including the intermittent system, compressor surface temperature, and local environment temperature. The pressure transducers were in the 0 ~ 3,447 kPa measurement range, except the discharge one was 0 ~ 6,894 kPa for safety concerns. There were two mass flow meters used. One was for the total mass flow rate, located right after the compressor discharge site, and the other measured the hot gas bypass mass percentage. Both mass flow meters had 0.11% reading accuracy. All the test instruments were calibrated before

installation in the test facility. Before acquiring the test data, the system was operated for one or two hours to reach the steady-state conditions, and then data was recorded every second for at least half an hour. The absolute uncertainty was then calculated by the root sum of squares (RSS) of the systematic error and random error

**Table 2:** Instruments and Uncertainties

| Instrument | Manufacturer / Model | Range | Systematic Uncertainty |
|---|---|---|---|
| RTD | Omega 1/10 DIN | -100 °C ~ 400 °C | $\pm 1/10 \times (0.3 + 0.005 \times t)$ °C |
| Thermal couple | Omega T Type | -200 °C ~ 200 °C | $\pm 0.5$ °C |
| Pressure transducer | Setra 280E | 0 ~ 3,447 kPa | $\pm 0.11\%$ FS |
| Pressure transducer | Setra 280E | 0 ~ 6,895 kPa | $\pm 0.11\%$ FS |
| Mass flow meter | Micro Motion 2700+CMFS025M | 0 ~ 310 g/s | $\pm 0.35\%$ of reading |
| Wattmeter | Ohio Semitronics GH-020D | 0 ~ 4,000 W | $\pm 0.2\%$ of reading |

## 3.2 Test Matrix

Based on the observation by Lee et al. (2021), the mass flow rate of a fixed-speed rotary compressor can deviate by 60% under low ambient temperature. A test matrix covering wide operating conditions is necessary to evaluate the efficacy of this mixture prediction method. Figure 3 presents the comprehensive compressor test matrix for this work. The condensing temperature ranges from 25°C to 60°C and -30°C to 15°C for the evaporating temperature. The superheat 11 K was applied to all test points. The ambient temperature of the test facility was set to 25°C
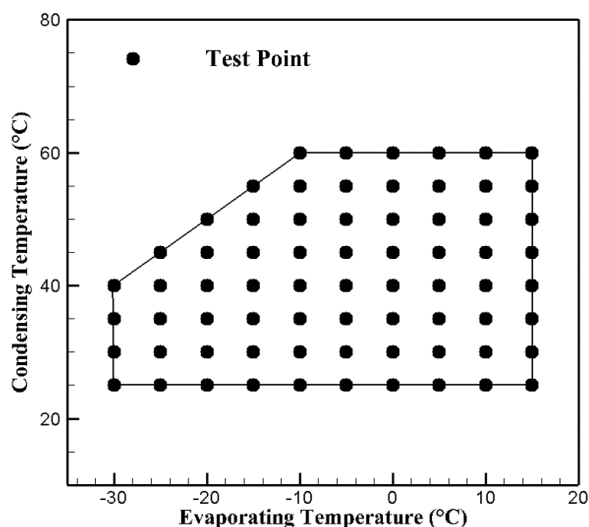


**Figure 3:** Test matrix

## 3.3 Compressor Specification

An R-410A inverter compressor was adopted to be tested and installed onto the test facility. The displacement was 10.2 ml/rev, and it was taken to calculate each condition's ideal mass flow rate. The rotation speed was set to 3,600 rpm through the inverter board. In addition, the lubricant oil was POE 68.

## 4. TEST RESULTS AND DISCUSSION

### 4.1 Single Point Prediction

According to the observations that the single-phase mixture flow in the clearance turned into a two-phase flow because of pressure drop, we can expect that the larger the pressure drop, the more noticeable the phenomenon. While we adopted the isothermal, single-phase mixture flow model, the reference test point should be in the middle of the test matrix to avoid the exacerbated impact of the bubbly flow. Therefore, the evaporating/condensing temperature (-5°C/45°C) was chosen to predict the whole test matrix.

As for the refrigerant oil flow properties, the oil sump temperature is critical to the solubility and viscosity. Nevertheless, no temperature sensor was monitoring the oil sump temperature. We assumed the mixture's temperature to be 60°C for all test points. And the kinematic viscosity at the inlet and outlet of the clearance can be obtained by giving the discharge or suction pressure together with the mixture's temperature. By averaging the kinematic viscosity of the inlet and outlet flows, we can estimate the kinematic viscosity of the mixture flow in the clearance.

When the reference point was chosen, the mass flow rate difference between the ideal mass flow rate, calculated based on displacement, and the actual mass flow rate was attributed to mixture leakage. As the refrigerant was degassing from the oil, the amount of mixture leakage can be calculated employing solubility difference at the inlet and outlet of the clearance. And Eq. (5) can be utilized to derive the predicted mixture mass flow rate based on the reference point. Eq. (9) shows that the predicted mass flow rate was represented by subtracting the refrigerant leakage from the ideal mass flow rate. Then, the deviation between prediction and experimental results can be displayed in the parity plots of Figures 4 and 6.

$$\dot{m}_{predicted} = \rho_{suction} \times V_{Disp} \times 60Hz - \dot{m}_{oilmixture,P} \times (\omega_{inlet} - \omega_{outlet}) \qquad (9)$$

The left-hand side of Figure 4 shows the single test point prediction results. 34% of data were within a 5% deviation, and 66% of data were within a 10% deviation. As mentioned before, the mixture's temperature was critical to the prediction. The reference point can accurately predict the other test points, which were also at condensing temperature 45°C but varied at the evaporating temperature, for about 1% to 2% deviation. But it failed to predict other condensing temperature cases and deviated most at higher condensing temperatures, 55°C, and 60°C.



(a)  Single Point Prediction                           (b) Two Points Prediction
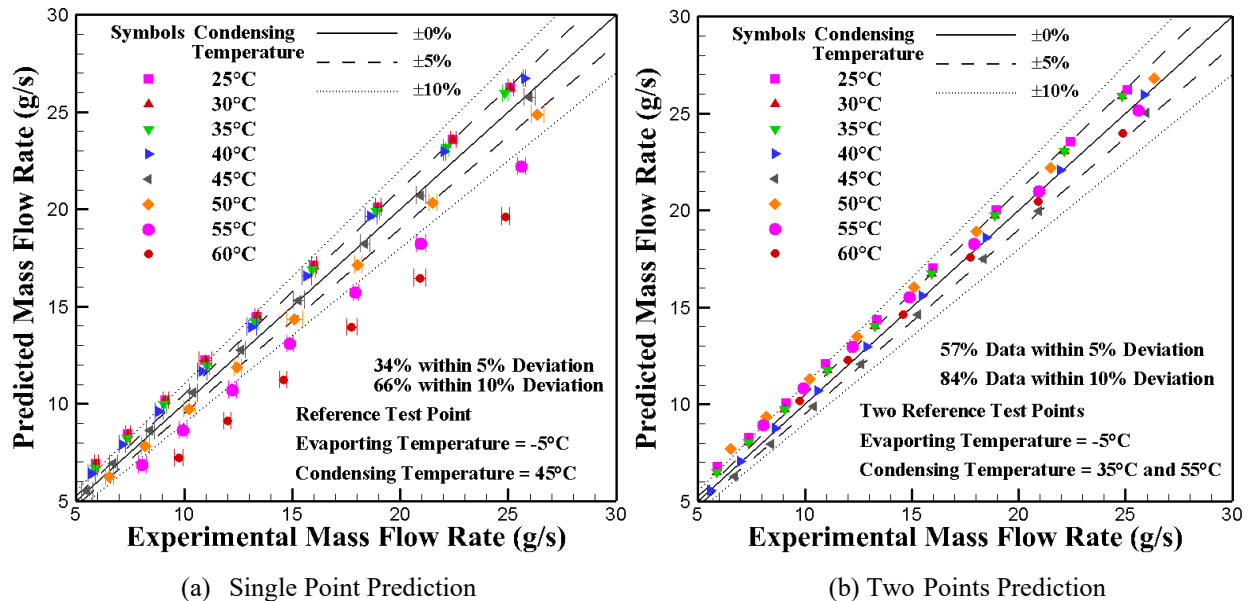
**Figure 4:** Single point and two points predicted MFR against the experimental MFR

### 4.2 Two Points Prediction

The left-hand side of Figure 4 shows that the single reference test point cannot fully capture significantly changing properties in the higher condensing temperature range. Therefore, we split the test matrix into higher and lower condensing temperature zones. Like the previous section, we assigned each a center reference point to predict these two zones' mass flow rate, as shown on the right-hand side of Figure 4.
The condensing/evaporating temperature (-5°C,35°C) was assigned to predict the condensing temperature ranges from 25°C to 45°C, and point (-5°C, 55°C) was assigned to predict the condensing temperature from 50°C to 60°C. A significant improvement has been achieved. The prediction within 5% deviation data was improved from 34% to 57%, and the prediction within 10% deviation data was improved from 66% to 84%.

### 4.3 Variable Oil Sump Temperature Prediction

If we keep increasing the reference test points, the prediction results can be more accurate. The reason is that the reference mixture properties are closer to the predicted conditions. Therefore, it is crucial to determine and predict the mixture's temperature, which was cranked up from the oil sump, instead of increasing the reference points. A different approach to deciding the oil mixture temperature is discussed here. Figure 5 presents the discharge temperature against the pressure difference between discharge and suction pressure. Under the same condensing temperature, when the pressure difference decreases, the discharge temperature decreases less and less and flattens at the lower pressure difference—the smaller the pressure difference, the smaller the discharge temperature lift caused by the compression process. Therefore, assuming that the oil mixture temperature is close to the discharge temperature when the pressure difference is small enough is reasonable. The regression line between oil mixture temperature and the condensing temperature is shown in Figure 5.
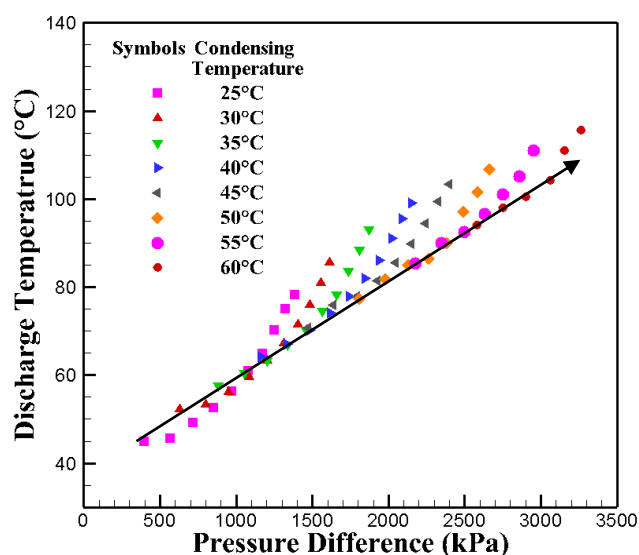


**Figure 5:** Pressure difference vs. discharge temperature

Following the assumption above, the regression correlation between mixture temperature and condensing temperature is as Eq. (10):

$$T_{oilmixture} = 1.4 \times T_{Condensing} + 10 \tag{10}$$

Instead of assigning the mixture's temperature like one point and two points prediction, the oil mixture temperature was set to be the function of condensing temperature, as Eq. (10) shows. Limited by the applicable range of the mixture properties correlation, 0°C < T < 75°C, the mixture properties for the condensing temperature 50°C, 55°C, and 60°C falls outside of the applying range and won't work. Therefore, these three condensing temperatures won't be compared in Figure 6.

In addition, using the variable temperature for viscosity resulted in a poor prediction against the experimental data. Because the kinematic viscosity was highly sensitive to the temperature change, the variable oil sump temperature displayed a more significant variation in kinematic viscosity. On the contrary, utilizing the fixed temperature model demonstrated better prediction results. The kinematic viscosity appeared unaffected by the temperature of the inlet mixture but was more affected by the suction side conditions. More studies of the mixture viscosity in the clearance are needed to describe such observations. The temperature of the mixture viscosity was set at 60°C for the time being. And the mixture solubility followed the variable oil sump temperature. The predicted mass flow rate can be obtained using Eq. (5) and Eq. (9), the same as the single point and two points prediction.

The single reference test point results were on the left-hand side of Figure 6. All the prediction points were within the 10% deviation, and 81% of prediction data were within the 5% deviation. The promising results indicate that the assumption of the mixture temperature is reasonable. As for the manufacturer's performance map, the inverter compressor was designed for multiple applications, including air-conditioner and heat pump units. Hence it covered a wide range of operating conditions and delivered an excellent prediction capability. The right-hand side of Figure 6 shows that 90% of the prediction points were within 10% deviation, and 67% of the data were within 5% deviation.

Compared to the manufacturer's map, the varied oil-sump single-point prediction had even better results, demonstrating the feasibility of mass flow rate prediction and indicating how to improve the prediction accuracy.
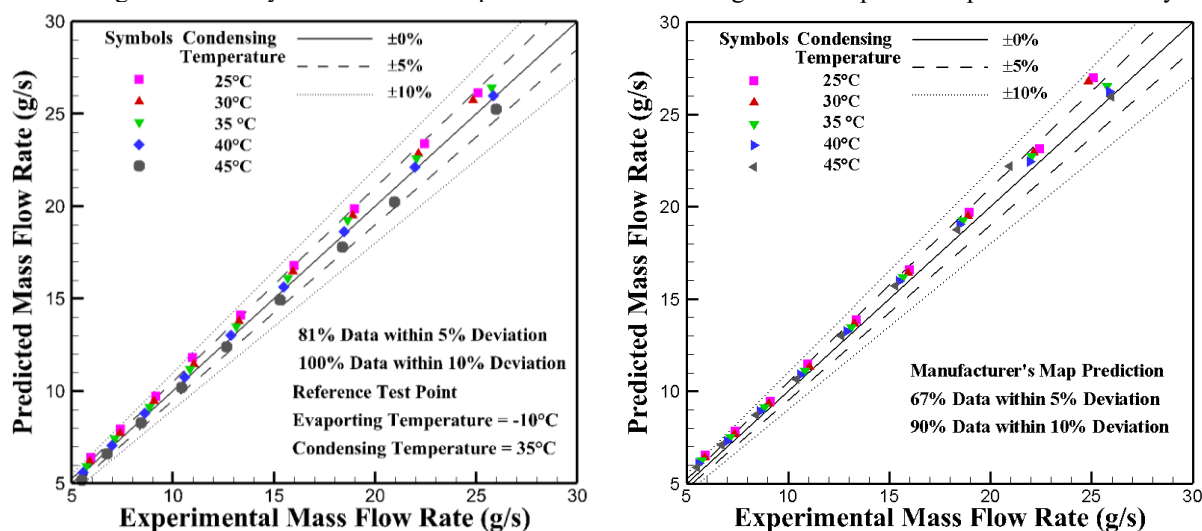


**Figure 6:** Varied Oil mixture temperature prediction and manufacturer's map

## 5. CONCLUSION

An improved mass flow rate prediction method was proposed for the rolling piston type compressor. Based on the visualization experiment done by Costa et al. (1990), the clearance was sealed with the oil mixture. And the refrigerant loss was attributed to the outgassing refrigerant from the oversaturated mixture. By identifying the critical affecting factors in the governing equations, the oil-mixture leakage can be predicted by correlating the pressure difference of the discharge and suction pressure and the mixture's kinematic viscosity with a reference test point mass flow rate.

A self-built compressor test facility was developed utilizing the hot gas bypass method to prove the idea is workable. The high-accuracy RTD, pressure transducer and mass flow meters deliver reliable and accurate measurements. The test matrix included a wide range of operating conditions and can be compared with the compressor manufacturer's map prediction.

Assuming the mixture was an isothermal model and the temperature was 60°C, the one-point reference prediction had 34% within 5% deviation and 66% within 10% deviation against the experimental results. That is because the one-point prediction cannot fully capture the properties change when the predicted properties are too digressed from the reference point. As a result, we divided the test matrix into upper and lower zones based on condensing

temperature, and each of these zones was predicted separately by each reference point. The prediction accuracy improved to 57% within 5% deviation and 84% within 10% deviation.

In place of assigning a mixture temperature, a varied oil sump temperature was regressed from the discharge temperature and applied to the single test point prediction. The results show that 81% of data are within 5% deviation, and 100% of data are within 10% deviation. The promising results demonstrated that further study of the oil sump temperature prediction could benefit this mass flow rate prediction method.

## NOMENCLATURE

| | | |
|---|---|---|
| m | mass | kg |
| P | pressure | Pa |
| T | temperature | K or °C |
| u | velocity in x-direction | m·s$^{-1}$ |
| v | velocity in y-direction | m·s$^{-1}$ |
| $V_{Disp}$ | displacement volume | ml |
| x | x coordinate | m |
| y | y coordinate | m |

**Greek symbols**

| | | |
|---|---|---|
| ρ | density | kg·m$^{-3}$ |
| μ | dynamic viscosity | Pa·s |
| ν | kinematic viscosity | mm2·s$^{-1}$ |
| ω | solubility | kg refrigerant/kg mixture |
| α | mass fraction | kg refrigerant/kg mixture |

**Subscript**

| | |
|---|---|
| oil mixture | oil mixture |
| P | predicted point |
| R | reference point |
| suction | suction |
| inlet | inlet |
| outlet | outlet |

## REFERENCES

Cai, D., He, G., Yokoyama, T., Tian, Q., Yang, X., & Pan, J. (2015). Simulation and comparison of leakage characteristics of R290 in rolling piston type rotary compressor. International Journal of Refrigeration, 53, 42-54.

Cai, D., Qiu, C., Pan, J., Yang, X., He, G., Tetsuhide, Y., ... & Li, H. (2017). Leakage characteristics and an updated volumetric efficiency prediction model of rolling piston type rotary compressor for small capacity air-conditioner and heat pump applications. Applied Thermal Engineering, 121, 1080-1094.

Castro, H. O. S., & Gasche, J. L. (2006). Foam flow of oil-refrigerant R134a mixture in a small diameter tube. In International Heat Transfer Conference 13. Begel House Inc.

Costa, C.M.N. F.; Ferreira, R. T. S.; and Prata, A. T., "Considerations About the Leakage Through the Minimal Clearance in a Rolling Piston Compressor" (1990). International Compressor Engineering Conference. Paper 780.

Dias, J. P., Gasche, J. L., & Seixlack, A. L. (2011). Mathematical modeling of the Ester oil-refrigerant R134a mixture two-phase flow with foam formation through a small diameter tube. Journal of the Brazilian Society of Mechanical Sciences and Engineering, 33(3), 314-323.

Gasche, J. L., Andreotti, T., & Maia, C. R. M. (2012). A model to predict R134a refrigerant leakage through the radial clearance of rolling piston compressors. International Journal of Refrigeration, 35(8), 2223-2232.

Henderson, D. R. (1994). Solubility, viscosity, and density of refrigerant/lubricant mixtures. Final technical report,[1 October 1992--19 April 1994] (No. DOE/CE/23810-34). Spauschus Associates, Inc., Stockbridge, GA (United States).

Huff, H. J. (2003). Integrated compressor-expander devices for carbon dioxide vapor compression cycles. Ph.D. Thesis. University of Maryland, College Park.

Lee, C. Y., Cao, T., Hwang, Y., Radermacher, R., & Shaffer, S. (2021, September). Development of accurate and widely applicable compressor performance maps. In IOP Conference Series: Materials Science and Engineering (Vol. 1180, No. 1, p. 012041). IOP Publishing.

Lee, Janghee and Min, Tae Sik, "Performance analysis of rolling piston type rotary compressor " (1988). International Compressor Engineering Conference. Paper 615.

Li, Song; Carow, James; Bacellar, Daniel; and Martin, Cara, "Comparative Studies of Scroll and Rotary Compressors for US Market Heat Pumps and Air Conditioners" (2021). International Compressor Engineering Conference. Paper 2664.

Poiate Jr, E., & Gasche, J. L. (2006). Foam flow of oil-refrigerant R12 mixture in a small diameter tube. Journal of the Brazilian Society of Mechanical Sciences and Engineering, 28(4), 390-398.

Wang, B., Ding, Y., & Shi, W. (2018). Experimental research on vapor-injected rotary compressor through end-plate injection structure with check valve. International Journal of Refrigeration, 96, 131-138.

Wu, J., "A Mathematical Model for Internal Leakage in a Rotary Compressor" (2000). International Compressor Engineering Conference.Paper 1425.

Yanagisawa, T., & Shimizu, T. (1985). Leakage losses with a rolling piston type rotary compressor. I. Radical clearance on the rolling piston. International Journal of Refrigeration, 8(2), 75-84.

Yang, H., Qu, Z., Zhou, H., & Yu, B. (2011). Study on leakage via the radial clearance in a novel synchronal rotary refrigeration compressor. International Journal of Refrigeration, 34(1), 84-93.

## ACKNOWLEDGEMENT